A Progress Report

Entitled

Analytical Study of Twin-Jet Shielding

Development of 3-Dimensional Model

Submitted to

Noise Technology Branch
ANRD
NASA Langley Research Center

by

Carl H. Gerhold
Department of Mechanical Engineering
Texas A&M University
College Station, Texas 77843

November 4, 1980

TABLE OF CONTENTS

Analytical Study of Twin - Jet Shielding
Development of 3 - Dimensional Model

I SUMMARY

Previous project reports on the analytical study of twin-jet shielding have dealt with the formulation of the analytical model (1) and the solution of the model in two dimensions (2). The first report considered a point noise source impinging on a cylinder of heated flow. The solution reduces to an indefinite integral involving Bessel Functions. Methods to be investigated in order to solve the integral were outlined in the report. The second report discussed solution of the model consisting of a line source impinging on a cylinder of heated air. This two-dimensional approach eliminates the integral form of the solution. The trend of the estimated variation in shielding with frequency and azimuthal location was found to agree with the experimental data.

In the present report, the solution for a point source impinging on a cylinder of heated flow is presented. The indefinite integral is solved approximately using a saddle of point method. Comparison of the three-dimensional model to the previously obtained two-dimensional model, indicate that the approximate solution of the integral is valid.

The model is analysed in order to differentiate among the mechanims of shielding. The zones in which diffraction and transmission dominate are identified.

The model is found to compare to experimental shielding results. The major discrepancy between the model and experiment is felt to arise from the difference between the single point noise source of the model and the distributed source of the jet. Refinement of this noise source to a more realistic

representation of the real jet is one of the goals of the proposed continuation of this project (6).

Further work in the present project includes investigation of the effects of mach number, jet temperature and source/shielding jet separation on shielding.

II FORMULATION OF THE MODEL

The derivation of the model was shown in the first progress report (1). A summary of that derivation is shown below.

The mechanisms by which shielding occurs are reflection and refraction of sound at the boundary between the jet and the surrounding air and by diffraction around the jet.

The noise source is modelled by a stationary, discrete frequency point source located at $(r_o, \theta_o, 0_o)$. The shielding jet is a cylinder of radius a, and is infinite in extent along the z-axis. The temperature and flow velocity are uniform across the cylinder cross-section. The model is illustrated in Figure 1. The expression for acoustic velocity potential is written for two regions; region I is outside the jet, region II is within the jet.

In region 1 (outside the flow-incident upon the shielding jet)

$$\nabla^2\phi - \frac{1}{c_o^2}\phi_{tt} = Q_o e^{-i\omega t}\,\delta(r-r_o)\,\delta(\theta-\theta_o)\,\delta(z) \qquad 1a)$$

In region I (outside the flow-reflected from the shielding Jet)

$$\nabla^2\phi - \frac{1}{c_o^2}\phi_{tt} = o \qquad 1b)$$

In region II (inside the flow)

$$\nabla^2\phi - M^2\phi_{zz} - \frac{2M}{c_1}\phi_{zt} - \frac{1}{c_1^2}\phi_{tt} = o \qquad 2)$$

Where:

$(r_o, \theta_o, o,)$ - location of point source

(r, θ, z) - Location of the receiver

ω - Source frequency

Q_o - Source strength

c - sound speed

M - mach number - (jet flow speed/c_1)

$$\nabla^2\phi = \phi_{rr} + \frac{1}{r}\phi_r + \frac{1}{r^2}\phi_{\theta\theta} + \phi_{zz}$$

Note: The subscrip. refers to conditions outside the flow (ambient), and 1 refers to conditio. within the heated jet.

The boundary conditions at the interface between the ambient air and the jet are:

1) Pressure continuity

$$(p)_o = (p)_1 \quad \text{at } r = a$$

or-

$$-\rho_o(\phi_t)_o = -\rho_1(\phi_t + V\phi_z)_1 \quad \text{at } r = a \qquad 3)$$

2) Continuity of the vortex sheet (2). This condition states that the displacement of the medium is continuous and symmetrical at the boundary; r = a. Denoting this displacement by $\eta = (z,t)$, then:

$$\left.\frac{D\eta}{Dt}\right|_o = \left.\frac{D\eta}{Dt}\right|_1 \quad \text{at } r = a$$

or-

$$(\eta_t)_o = (\eta_t + V\eta_z)_1, \quad \text{at } r = a \qquad 4)$$

Time is eliminated from equations 1 and 2 by assuming:

$$\phi(r, \theta, z, t) = \psi(r, \theta, z)e^{-i\omega t}$$

The problem is reduced to a two-dimensional formulation by the Fourier transform:

$$\tilde{\psi} = \frac{1}{2\pi}\int_{-\infty}^{+\infty} \psi e^{-ik_z z}\, dz$$

with corresponding inverse:

$$\psi = \int_{-\infty}^{+\infty} \tilde{\psi} e^{ik_z z} dk_z$$

Solution of the transformed equations, inclusion of the boundary conditions and inverse transformations yields the equation for the acoustic velocity potential in the far field (r>>a):

$$\phi = \frac{-iQ_o e^{-i\omega t}}{8\pi} \sum_{m=0}^{\infty} \epsilon_m \cos m(\theta-\theta_o) \int_{-\infty}^{+\infty} H_m(K_o r)\, F_m(K_o,K_1) e^{ik_z(z)} dk_z \qquad 5)$$

where:

$$F_m(K_o,K_1) = J_m(K_o r) - \frac{H_m(K_o r_o)[J_m(K_1 a)J_m'(K_o a) - TJ_m(K_o a)J_m'(K_1 a)]}{TH_m(K_o a)J_m'(K_1 a) - J_m(K_1 a)H_m'(K_o a)]}$$

$$T = \frac{k_o^2\ c_o^2\ \rho_o k_1}{k_1^2\ c_1^2\ \rho_1 K_o}$$

$$k_o = \omega/c_o$$

$$k_1 = (\frac{\omega}{c_1} - Mk_z)$$

$$K_o = [k_o^2 - k_z^2]^{1/2}$$

$$K_1 = [k_1^2 - k_z^2]^{1/2}$$

III SOLUTION OF THE MODEL

An approximate solution of the integral in equation 5 is obtained using the Method of Stationary Phase (3). By this method, the solution of the integral I_z, of the form:

$$I_z = \int_{-\infty}^{+\infty} g(\alpha) e^{iz(h(\alpha))} d\alpha \quad \text{as } z \to \infty \qquad 6)$$

is:

$$I_z = \left[\frac{2\pi}{z \left| h''(\alpha_o) \right|} \right]^{\frac{1}{2}} g(\alpha_o)\, e^{i(z(h(\alpha_o)) \pm \pi/4)} \qquad 7)$$

where:

1) α_o solves $h'(\alpha) = 0$

2) the sign in the exponential term goes as the sign of $h''(t_o)$

In order to solve equation 5 in the manner prescribed by equation 6, the following transformations are made.

Let:

$$\alpha = \sqrt{1 - \left(\frac{k_z}{k_o}\right)^2}$$

then:

1) $dk_z = -\dfrac{k_o \alpha \, d\alpha}{\sqrt{1-\alpha^2}}$

2) $k_1 = \dfrac{\omega}{c_1} - Mk_z = k_o \left(\dfrac{c_o}{c_1} - M\sqrt{1-\alpha^2} \right)$

3) $K_o = [k_o^2 - k_z^2]^{\frac{1}{2}} = k_o \alpha$

4) $K_1 = [k_1^2 - k_z^2]^{\frac{1}{2}} = k_o \left[\left(\dfrac{c_o}{c_1} - M\sqrt{1-\alpha^2} \right)^2 - 1 + \alpha^2 \right]^{\frac{1}{2}}$

the integral in equation 5 :

$$I = \int_{-\infty}^{+\infty} e^{ik_z z} H_m(k_o r)\, F_m(k_{o_1} k_1) \quad dk_z$$

becomes:

$$I = -k_o \int_{-\infty}^{+\infty} \frac{\alpha e}{\sqrt{1-\alpha^2}}^{ik_o z \sqrt{1-\alpha^2}} H_m(k_o r\alpha)\, F_m(\alpha)\, d\alpha \qquad 8)$$

In the acoustic far field, r>>1. Assuming that $k_z << k_o$, the argument of the Hankel function becomes large:

$$k_o r\alpha >> 1$$

and the Hankel function is approximated by:

$$H_m(k_o r\alpha) \approx \sqrt{\frac{2}{\pi\, k_o r\alpha}}\; e^{i(k_o r\alpha - \frac{\pi}{2}(m + \frac{1}{2}))} \qquad 9)$$

from figure 1, it is seen that:

$$r = R \cos\beta \text{ and } z = R \sin\beta$$

where:

R = distance from origin of the coordinate system to the receiver

β = angle between vector R and the projection of the vector R on the x - y plane.

The integral is then:

$$I = -\sqrt{\frac{2k_o}{\pi R \cos\beta}}\, (e^{-i\frac{\pi}{2}(m + \frac{1}{2})}) \int_{-\infty}^{+\infty} e^{ik_o R(\sqrt{1-\alpha^2}\sin\beta + \alpha\cos\beta)} \sqrt{\frac{\alpha}{1-\alpha^2}}\, F_m(\alpha)\, d\alpha \qquad 10)$$

comparing equation 10 to equation 6 :

$$z = k_o R$$

$$h(\alpha) = \sqrt{1-\alpha^2}\sin\beta + \alpha\cos\beta$$

$$g(\alpha) = \sqrt{\frac{\alpha}{1-\alpha^2}}\, F_m(\alpha)$$

α_o is evaluated from:

$$h'(\alpha_o) = \cos\beta - \frac{\alpha_o}{\sqrt{1-\alpha_o^2}}\sin\beta = 0$$

thus:

$$\alpha_o = \cos\beta \qquad 11)$$

then: $h(\alpha_o) = 1$

and: $h''(\alpha_o) = -\frac{1}{\sin^2\beta}$

and: $g(\alpha_o) = \sqrt{\frac{\cos\beta}{\sin^2\beta}}\, F_m(\cos\beta)$

The integral, as $k_o R \gg 1$, becomes:

$$I = \frac{2i}{R} e^{-im\pi/2} e^{ik_o R} F_m(\cos\beta) \qquad 12)$$

From which the expression for the far field acoustic velocity potential is evaluated:

$$\phi = \frac{Q_o e^{-i\omega t}}{4\pi R} \sum_{m=0}^{\infty} \epsilon_m \cos m(\theta-\theta_o) e^{\frac{-im\pi}{2}} e^{ik_o R} F_m(\cos\beta) \qquad 13)$$

Where:

$$F_m(\cos\beta) = J_m(k_o r_o \cos\beta) -$$

$$\left\{ H_m(k_o r_o \cos\beta) \left[\rho_1 c_1^2 T_1^2 \cos\beta\, J_m(k_o a T_2)\, J_m'(k_o a \cos\beta) \right.\right.$$

$$\left. - \rho_o c_o^2 T_2\, J_m(k_o a \cos\beta)\, J_m'(k_o a T_2) \right] /$$

$$\left. \left[\rho_1 c_1^2 T_1^2 \cos\beta\, J_m(k_o a T_2)\, H_m'(k_o a \cos\beta) - \rho_o c_o^2 T_2\, H_m(k_o a \cos\beta)\, J_m'(k_o a T_2) \right] \right\} \quad 14)$$

where:

$$T_1 = \frac{c_o}{c_1} - M \sin\beta$$

$$T_2 = \left[\left(\frac{c_o}{c_1} - M \sin\beta \right)^2 - \sin^2\beta \right]^{\frac{1}{2}}$$

The total acoustic velocity potential in the far field consists of two parts:

1. The velocity potential of the incident wave:

$$\phi_{in} = \frac{Q_o e^{-i\omega t}}{4\pi R} \sum_{m=o}^{\infty} \epsilon_m \cos m(\theta - \theta_o) e^{\frac{-im\pi}{2}} e^{ik_o R} J_m(k_o r_o \cos\beta) \quad 15)$$

2. The velocity potential of the scattered wave:

$$\phi_{sc} = \frac{Q_o e^{-i\omega t}}{4\pi R} \sum_{m=o}^{\infty} \epsilon_m \cos m(\theta - \theta_o) e^{\frac{im\pi}{2}} e^{ik_o R} X$$

$$\left\{ \text{terms in equation 14) within brackets} \right\} \quad 16)$$

As a check; when $r_o = o$ (source is located at the origin), the velocity potential of the incident wave reduces to:

$$\phi_{in} = \frac{Q_o e^{ik_o(R-ct)}}{4\pi R}$$

since;

$$J_m(o) = \begin{cases} 1 & m = o \\ o & m \neq o \end{cases}$$

This is the expression for the velocity potential in the far field for radiation from a point source of strength, Q_o, located at the origin of the co-ordinate system.

IV RESULTS

The total sound pressure is evaluated from the acoustic velocity potential by:

$$P_T = -\rho_o \frac{\partial \phi}{\partial t} T$$

The incident sound pressure is evaluated from equation 15:

$$P_{in} = -\rho_o \frac{\partial \phi_{in}}{\partial t} = + \frac{i\omega Q_o}{4\pi R} \rho_o \sum_{m=o}^{\infty} \epsilon_m \cos m(\theta-\theta_o) e^{\frac{-im\pi}{2}} e^{ik_o R} J_m(k_o r_o \cos \beta) \quad 17)$$

The normalized sound pressure is formed from the magnitude of the ratio of the total sound pressure to the incident sound pressure. This normalized sound pressure is a measure of the influence of the shielding jet on the noise source directionality. A value of normalized sound pressure less that one indicates noise reduction; and a value of normalized sound pressure greater than one indicated amplifications.

1. Comparison of 3 - dimensional Model to 2 - dimensional Mod

The 3 - dimensional model is compared to the 2 - dimensional model developed in a previous report (2). The conditions imposed are:

a) M = Mach number = 0.0

b) β = 0.0

c) $\theta-\theta_o = \pi$

Under these conditions, the receiver is located in the x-y plane of the source, on the side of the jet opposite the source. It is expected that the normalized sound pressure reduces to the two dimensional case investigated in a previous progress report (2). The results obtained are shown in figure 2 and are compared to plots obtained previously. The plots of normalized sound

pressure against non-dimensional frequency parameter, $k_o a$, are comparable from the two studies. This indicates that the approximation of the integral employed in the present study is valid.

2. Variation of Normalized Sound Pressure with Angle to Jet Axis.

In order to differentiate among the mechanisms of shielding, the normalized sound pressure is evaluated at low frequencies under the following operating conditions.

a) V_J = Jet velocity = 1552 feet/sec

b) T_J = Jet temperature = 1238°R

c) T_o = Ambient temperature = 530° R

d) S/D = Spacing parameter = ratio of distance from source to center of jet and jet diameter. = 2.67

The normalized sound pressure is evaluated in the shielded zone of the jet. Thus, $\theta-\theta_o = \pi$ and $o \leq \beta < \pi/2$. For the purposes of comparison to other data, the coordinates are shifted to a set centered in the source, and illustrated in figure 3. In the nomenclature adopted in the figure, $\psi_n = o°$ is on the z-axis of the noise source, and $\psi = 90°$ is on the side of the jet directly opposite the source.

The contours of normalized pressure for $10° \leq \psi_n \leq 90°$ are plotted against non-dimensional frequency parameter in figure 4. The non-dimensional frequency $k_o a$ is varied from 0.1 to 1.0.

At angles close to the z-axis of the noise source, $10° < \psi_n < 40°$, the effect of increasing the angle is to shift the normalized sound pressure curve to lower frequencies. As the angle increases, the line of sight distance from the source to the jet becomes smaller. From barrier theory arguments developed in a previous report (2), the expected result of decreasing the spacing between the

source and the shielding jet is to increase the attenuation of the lower frequency sounds. Thus, in the range $10° < \psi_n < 40°$, diffraction around the jet dominates.

In the range of incident angles $40° < \psi_n < 90°$, the trend reverses, and increasing the angle of incidence shifts the curves toward higher frequencies. In this range, the sound transmitted through the jet is combining with the diffracted sound. This conclusion is consistent with analysis by Yeh (5). Yeh considered a sound ray incident upon a uniform sheet of thickness, D, in which the flow and temperature are constant. The sound ray is inclined at an angle ψ_n to the axis of the flow sheet. The model is illustrated in figure 5 . The temperature difference and flow cause the incident sound ray to be refracted, with the angle in the jet, ψ_J, evaluated from:

$$\cos \psi_J = \frac{C_J \cos \psi_n}{C_o - V_J \cos \psi_n}$$

Transmission through the jet is minimized when the refracted ray becomes parallel to the jet or $\psi_J = o$. The critical value of the incident ray, ψ_{nc}, corresponding to $\psi_J = o$ is:

$$\cos \psi_{nc} = \frac{C_o}{C_J + V_J}$$

The jet parameters:

$$C_o = 1128 \text{ feet/sec}$$

$$C_J = 1725 \text{ feet/sec}$$

$$V_J = 1552 \text{ feet/sec}$$

result in:

$$\psi_{nc} = 69.9°$$

Yeh's model estimates that all the incident sound in the range $\psi_n > \psi_{nc}$ is transmitted through the jet, while no transmission occurs for sound incident at an angle $\psi_n < \psi_{nc}$.

Referring to figure 4, the normalized sound pressure decreases more rapidly in the range of angles $40° < \psi_n < 70°$ than it does in the range $70° < \psi_n < 90°$. This indicates that sound incident at $\psi_n > 70°$ is transmitted through the jet; and that the contributions from the transmitted sound decreases rapidly for $\psi_n < 70°$. At angles of incidence, $\psi_n < 40°$, the diffracted sound contribution dominates.

3. Comparison to Experimental Results.

The analytical model is compared to experimental results by Kantola (4) and plotted in figure 6. The condition evaluated is:

a. $T_J = 1238°$ R

b. $V_J = 1519$ feet/sec

c. S/D = 2.67

d. $\psi_n = 30°, 60°$

The analytical model shows some agreement in form with the experimental data. The onset of shielding occurs at lower frequency for $\psi_n = 30°$ than it does for $\psi_n = 60°$. As the jet axis is approached, the agreement between the analytical and experimental improves, with the significant difference being at high frequencies. The analytical model shows that the normalized sound pressure increases for $k_o a > 10$. This indicates a upper frequency limit on shielding. The experimental results indicate no such upper limit in the range of frequencies investigated.

The major discrepancy between the analytical and experimental results occurs at greater angles of incidence. This is felt to be due to the point source approximation of the source jet. The jet noise source is more realistically

considered to be a distribution of point sources along the jet axis. The downstream sources are contributing to the sound pressure measured in the shielded zone. From the previous discussion on transmission though the shielding jet, the sound incident on the jet at $\psi_n > 70°$ is transmitted more readily than sound incident at $\psi_n < 70°$. In general then, sound is transmitted upstream more efficiently than downstream because the angle of incidence is greater. Thus, the receiver at $\psi_n = 60°$ "sees" more of the downstream noise sources than does the receiver located closer to the jet axis. The point source approximation for the source jet breaks down as the angle of incidence increases.

V. CONCLUSIONS

The 3 - dimensional model of twin jet noise shielding has been obtained for a point noise source impinging on a cylinder of heated flow. The validity of mathematical approximation required in the solution is tested by comparison of the 3 - dimensional model to a previously obtained 2 - dimensional formulation.

In the shielded zone, the normalized sound pressure curve is shifted toward higher frequencies as the angle of incidence from the jet axis is increased. This trend is expected from barrier theory. In this range of angles, diffraction around the jet dominates. For the jet parameters chosen, diffraction is the dominant mechanism for $\psi_n < 40°$. As the angle of incidence increases further, transmission of sound through the jet contributes to the diffracted sound. At angles of incidence greater than a critical value defined by:

$$\cos \psi_{nc} = \frac{C_o}{C_J + V_J}$$

Transmission through the jet is the dominant mechanism.

The analytical model compares to experimental results more favorably for angles of incidence close to the jet axis. The discrepencies that occur at greater angles of incidence are felt to arise from the difference between the single point source approximation in the model and the distributed source configuration of the real jet.

REFERENCES

L. Gerhold, C.; "Development of an Analytical Model of Twin Jet Shielding". Progress report or NASA Grant NAG-1-11. June 18, 1980

2. Gerhold, C.; "Analytical Study of Twin Jet Shielding - Two-Dimensional Model". Progress report for NASA Grant NAG-1-11. August 14, 1980

3. Jefferies, H. and Jefferies, B.; Methods of Mathematical Physics. Cambridge University Press, 1956

4. Kantola, R.A. "Shielding Aspects of Heated Twin Jet Noise", AIAA 4th Aeroacoustics Conference, Atlanta, Georgis, October 3-5, 1977

5. Yeh,C.; "A Further Note on the Reflection and Transmission of Sound Waves by a Moving Fluid Layer". Journal Acoustical Society of America vol. 43, no. 6, pp. 1454-1455, 1960

6. Gerhold,C.; "Analytical Study of Twin-Jet Shielding Progress to Date and Proposed Project Continuation". Progress report for NASA Grant NAG-1-11. October 1,1980

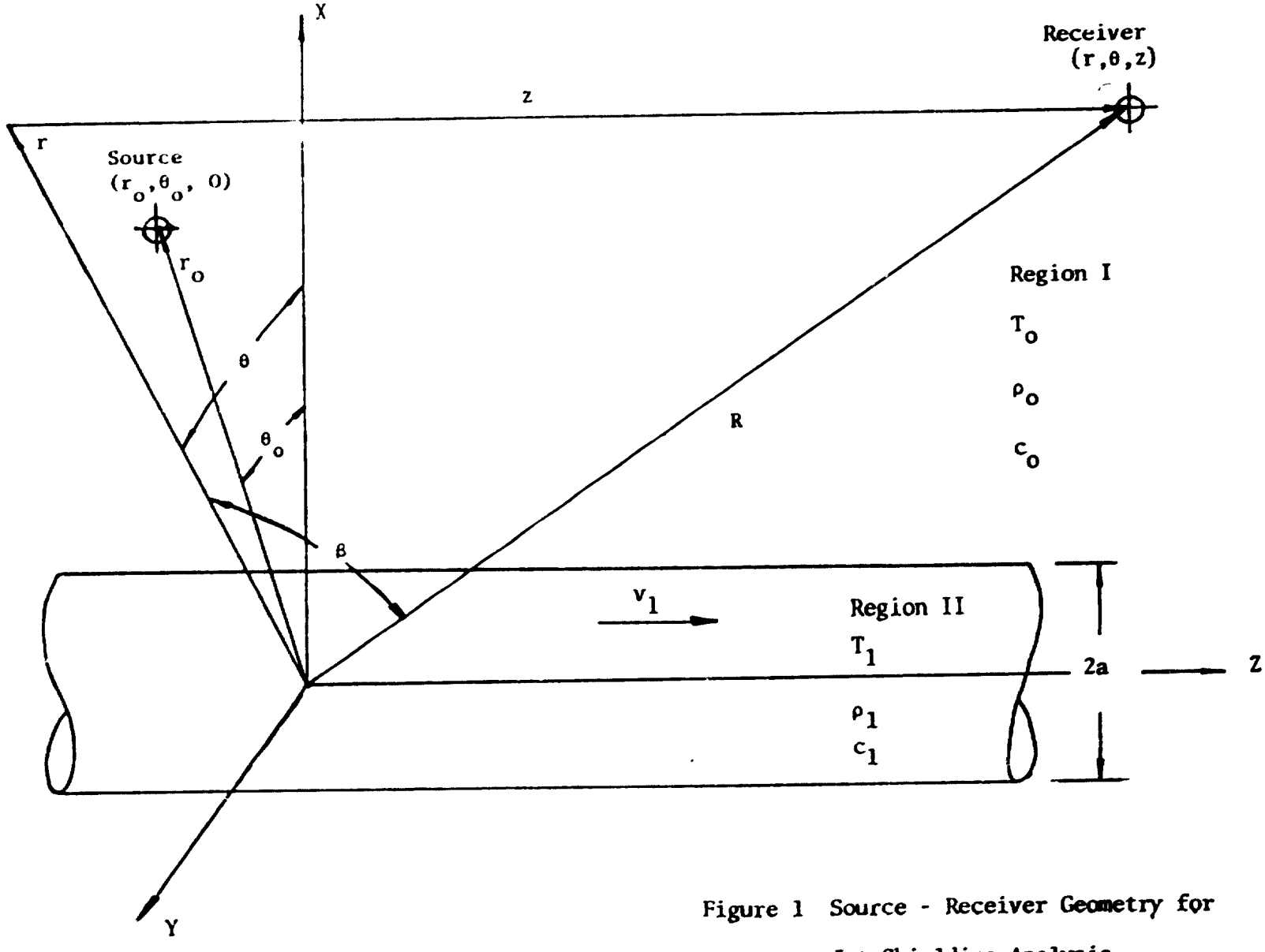

Figure 1 Source - Receiver Geometry for Jet Shielding Analysis.

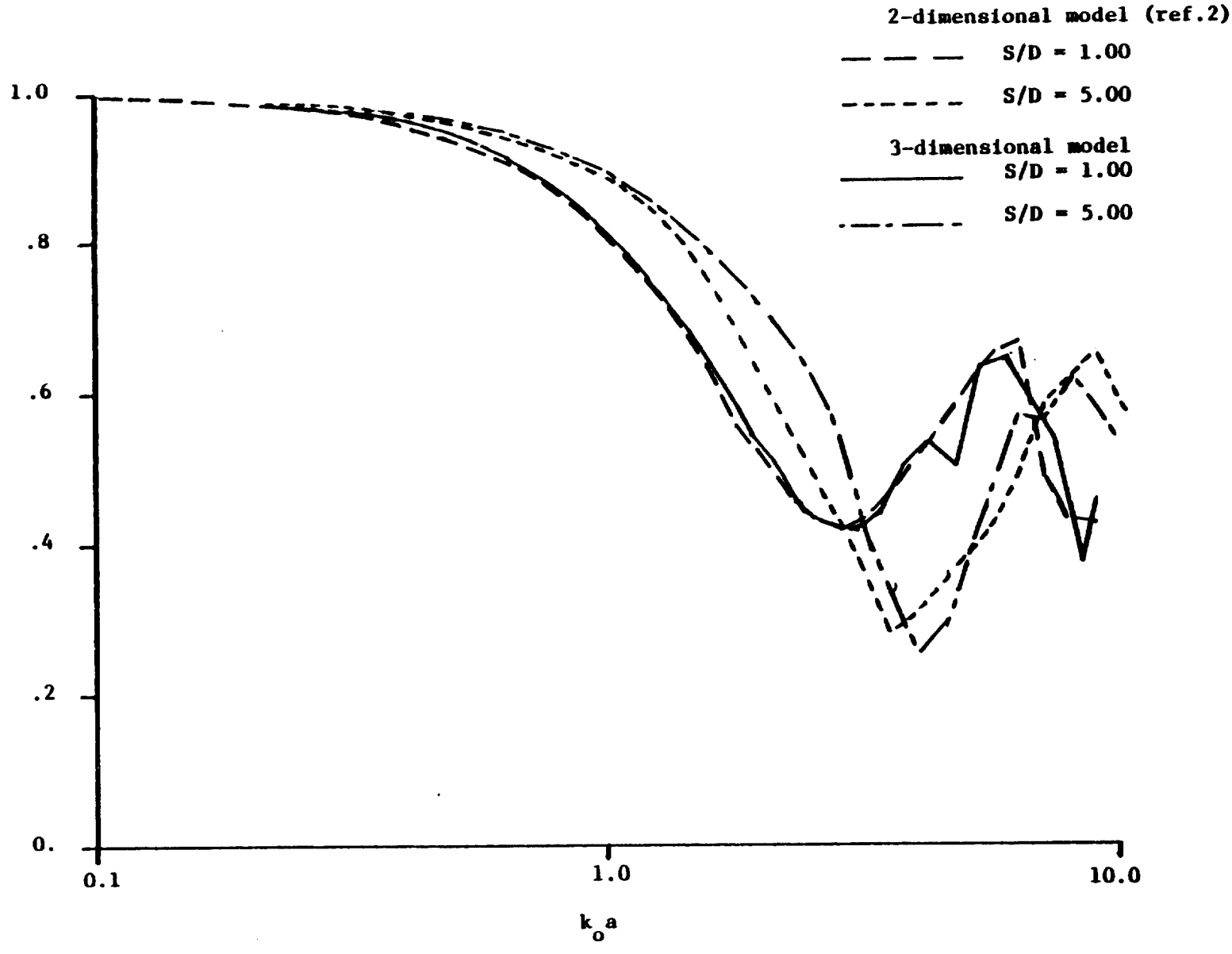

Figure 2. Variation of Normalized Sound Pressure with non-dimensional Frequency. Comparison of 2-dimensional model to 3-dimensional model.

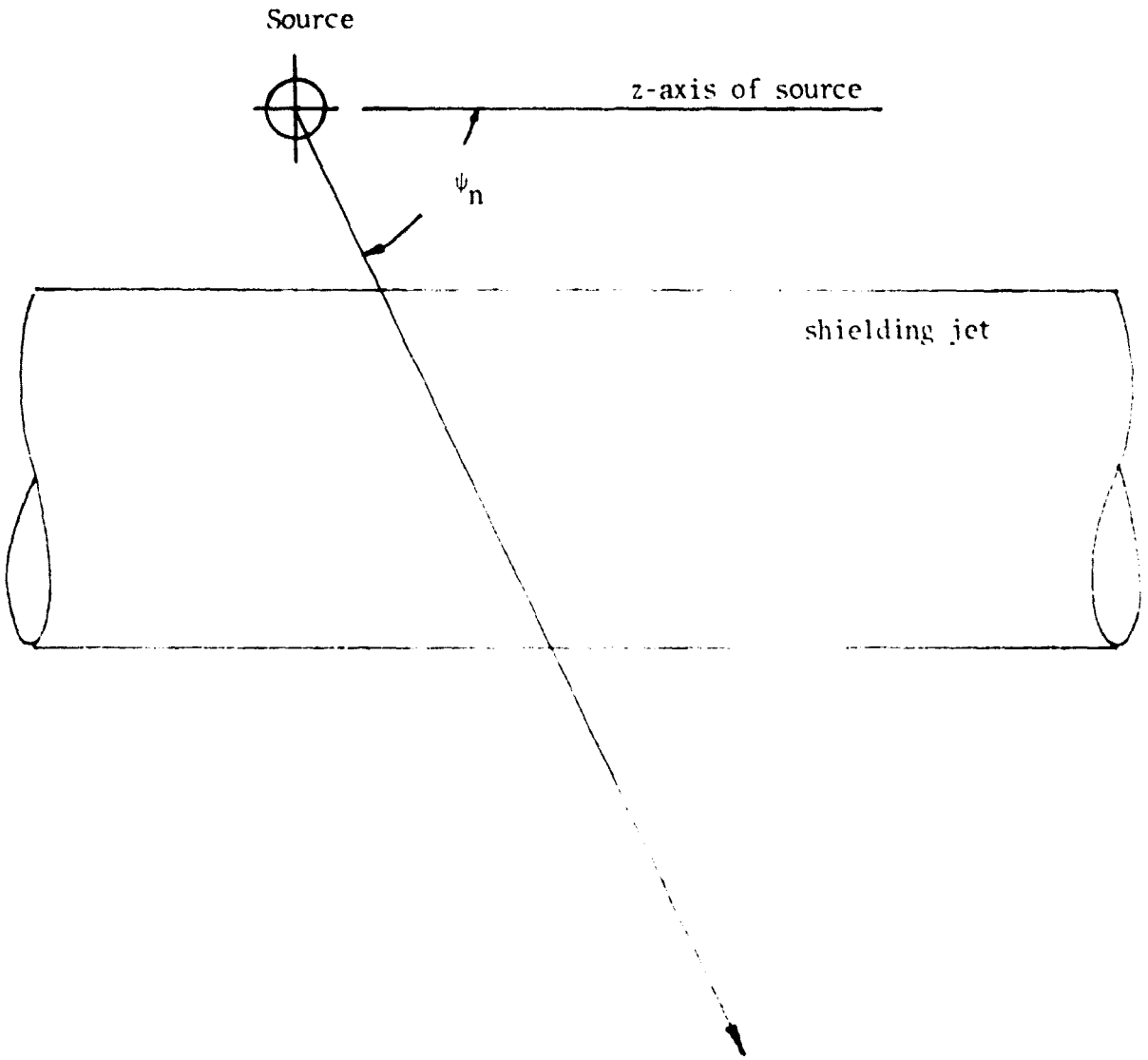

Figure 3 Definition of Angle in Coordinates centered on Noise source

Figure 4. Distribution of Normalized Sound Pressure in Shielded Zone.

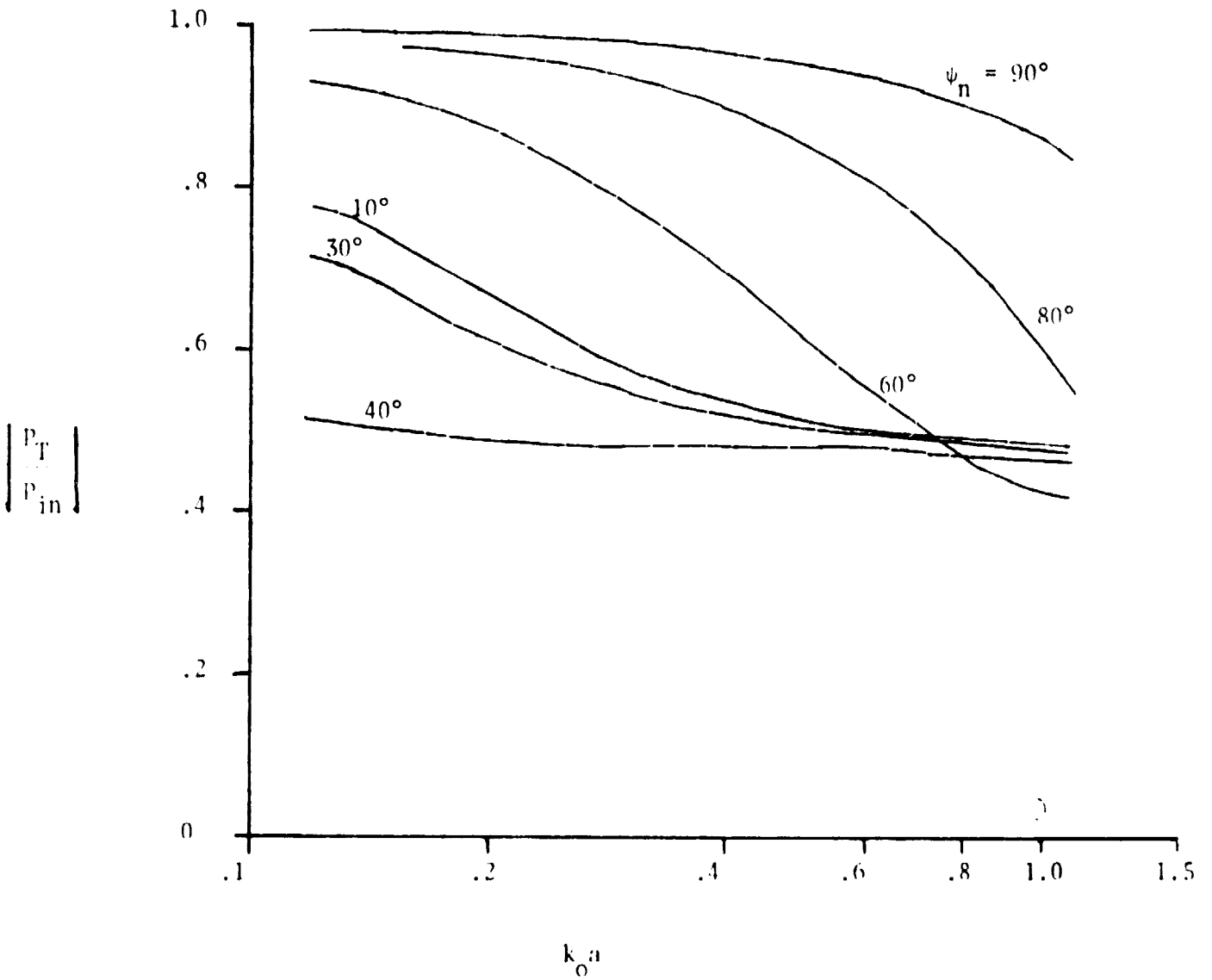

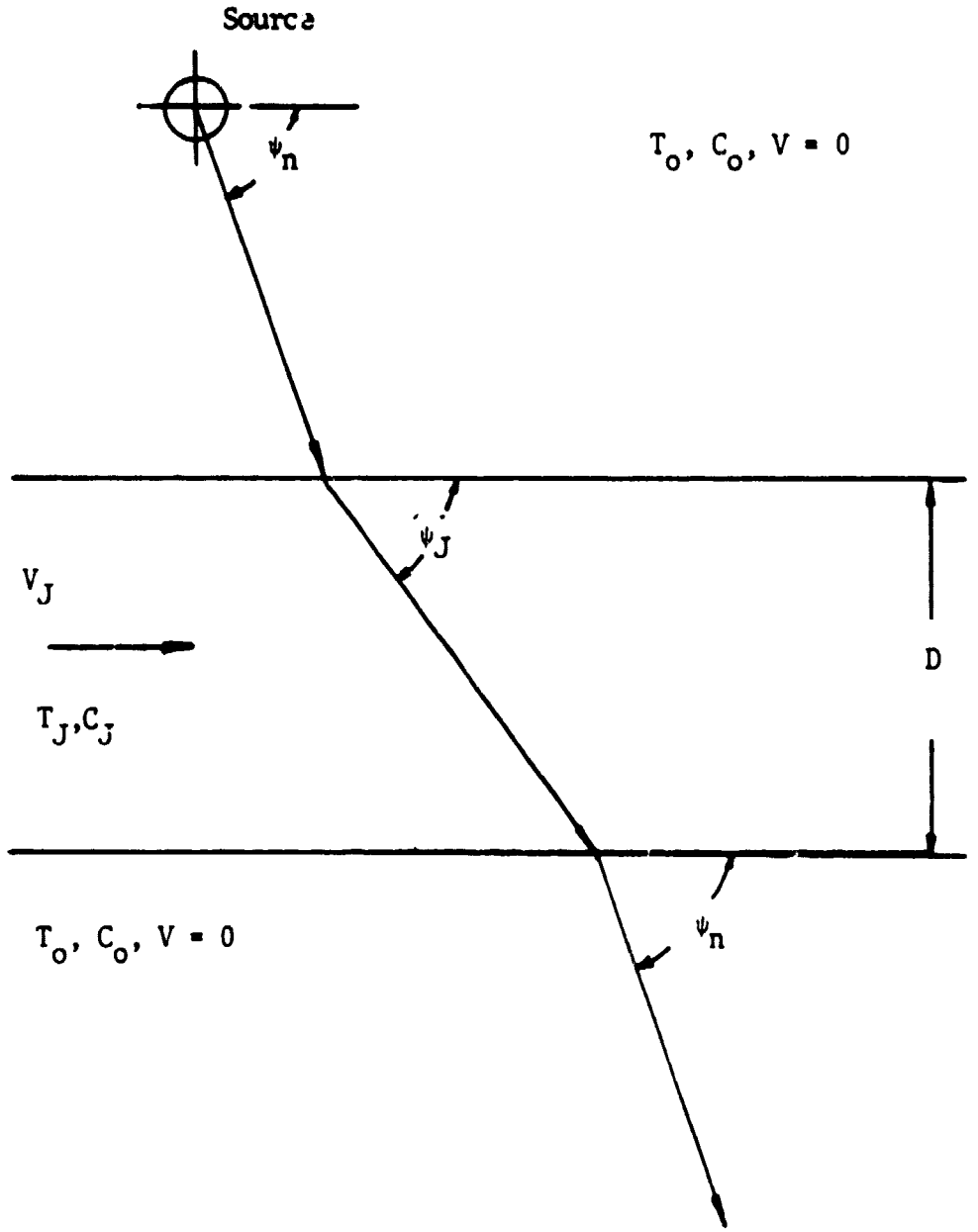

Figure 5. Sound Transmission Through Moving Heated Layer